IMMUNOMETABOLISM

A type 2 immune circuit in the stomach controls mammalian adaptation to dietary chitin

Do-Hyun Kim[1], Yilin Wang[1], Haerin Jung[1], Rachael L. Field[1], Xinya Zhang[1], Ta-Chiang Liu[1], Changqing Ma[1], James S. Fraser[2], Jonathan R. Brestoff[1], Steven J. Van Dyken[1]*

Dietary fiber improves metabolic health, but host-encoded mechanisms for digesting fibrous polysaccharides are unclear. In this work, we describe a mammalian adaptation to dietary chitin that is coordinated by gastric innate immune activation and acidic mammalian chitinase (AMCase). Chitin consumption causes gastric distension and cytokine production by stomach tuft cells and group 2 innate lymphoid cells (ILC2s) in mice, which drives the expansion of AMCase-expressing zymogenic chief cells that facilitate chitin digestion. Although chitin influences gut microbial composition, ILC2-mediated tissue adaptation and gastrointestinal responses are preserved in germ-free mice. In the absence of AMCase, sustained chitin intake leads to heightened basal type 2 immunity, reduced adiposity, and resistance to obesity. These data define an endogenous metabolic circuit that enables nutrient extraction from an insoluble dietary constituent by enhancing digestive function.

Dietary fiber intake is associated with a lower risk of metabolic disorders such as obesity (*1*, *2*) and type 2 immune activation has been implicated in metabolic homeostasis (*3*–*5*), but little is known about how degradation of specific fibers influences host immunity and metabolism. In mammals, digestion is initiated in the upper gastrointestinal (GI) tract and is facilitated by mechanical forces, neural feedback, and enzymatic activities that coordinate chemical and physical disruption of the food bolus before passage into the highly absorptive small intestine. Digestion is essential for nutrient extraction, which is evident in bariatric surgical approaches that counteract overnutrition by reducing or bypassing gastric digestion (*6*). Nutrient availability is also limited by dietary fiber enrichment because most bulky insoluble polysaccharides are resistant to digestion by mammalian enzymes and undergo only limited degradation by distal gut microbes (*7*). A notable exception is chitin (β-1,4-poly-*N*-acetylglucosamine). One of the most abundant natural polysaccharides on Earth, chitin is a component of arthropods and fungi and is an initiator of type 2 immune responses. We hypothesized that chitin is digested in a distinctive manner because widely conserved chitin [illegible] are encoded by both commensal microbes [illegible] mammals, particularly those that consume chitin (*8*–*13*).

Dietary chitin induces gastric distension and type 2 immune triggering

Chitin activates lung group 2 innate lymphoid cells (ILC2s) by means of interleukin-25 (IL-25), IL-33, and thymic stromal lymphopoietin (TSLP) (*14*). To test GI responses to dietary chitin, "YRS" mice that express reporter alleles for ILC2 signature genes arginase-1 (Yarg; *Arg1*^{YFP}, where YFP is yellow fluorescent protein), IL-5 (Red5; *Il5*^{tdTomato}), and IL-13 (Smart13; *Il13*^{hCD4}) on wild-type (WT) and IL-25, IL-33 receptor (IL-33R), and thymic stromal lymphopoietin receptor (TSLPR) triple-knockout (TKO) (*15*) backgrounds were fed with standard chow containing either cellulose (control) or chitin as fiber (Fig. 1A and table S1). We tested 5 to 20% chitin, which approximates the dietary composition of insectivorous mammals (*11*, *12*). Food intake was similar, and GI transit time was unaffected by diet. However, we observed marked gastric distention and greater stomach contents in chitin-fed versus control-fed mice (Fig. 1B and fig. S1, A and B), indicating that dietary fiber influences stomach retention and stretch. Gastric epithelium rapidly

[1]Department of Pathology and Immunology, Washington University School of Medicine, St. Louis, MO, USA. [2]Department of Bioengineering and Therapeutic Sciences, University of California San Francisco, San Francisco, CA, USA.
*Corresponding author. Email: svandyken@wustl.edu

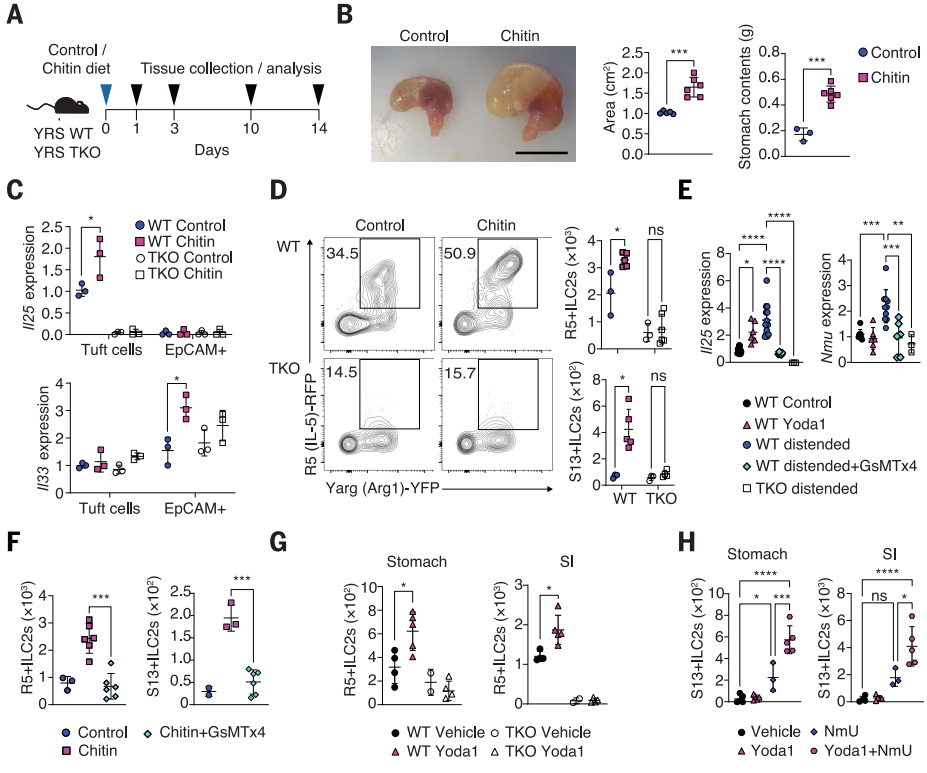

Fig. 1. Innate type 2 immune responses are triggered by gastric distension and dietary chitin. (**A**) Dietary responses in WT or TKO mice on triple-reporter (YRS) backgrounds. Representative stomach image (scale bar, 1 cm), stomach size, and luminal content (**B**); relative *Il25* and *Il33* expression in stomach tuft (CD45$^-$EpCAM$^+$SiglecF$^+$) and epithelial cells (CD45$^-$EpCAM$^+$) (**C**); and expression of R5 (*Il5*) and S13 (*Il13*) reporter alleles among stomach ILC2s (Yarg$^+$, pregated on CD45$^+$Lin$^-$Thy1.2$^+$) (**D**) in WT and TKO mice fed the indicated diet for 24 hours. RFP, red fluorescent protein. (**E**) Relative stomach gene expression in WT or TKO mice after Yoda1 administration or gastric distension. (**F**) R5 and S13 expression in stomach ILC2 after administration of the mechanosensitive ion-channel inhibitor GsMTx4 to mice fed the indicated diet for 12 hours. R5 (**G**) or S13 (**H**) expression in stomach and SI ILC2s after vehicle, Yoda1, and/or NmU administration. Data represent individual biological replicates except for the data in (C), which are pooled from two or three mice and are presented as means ± SD from two or more independent experiments ($n \geq 3$ mice per group). *P* values were calculated by unpaired *t* test [(B), (F), and (G)], one-way analysis of variance (ANOVA) [(E) and (H)], or two-way ANOVA with Tukey's multiple comparisons test [(C) and (D)]. **P* < 0.05; ***P* < 0.01; ****P* < 0.001; *****P* < 0.0001; ns, not significant.

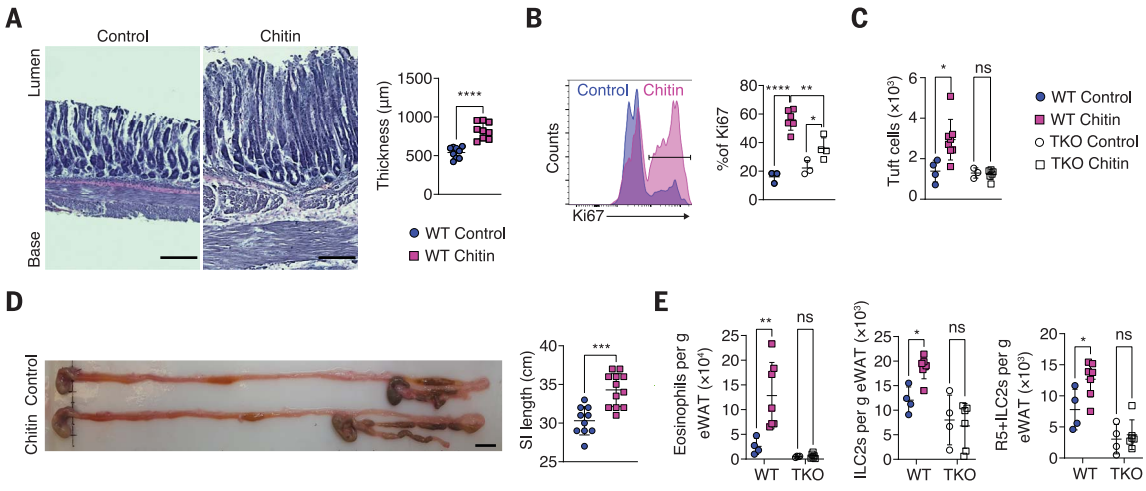

Fig. 2. Sustained chitin intake promotes GI remodeling and adipose ILC2 responses. Representative stomach histology images [hematoxylin and eosin (H&E) stained] (scale bars, 100 μm) (**A**), Ki67-expressing stomach epithelial cells (**B**), stomach tuft cells (**C**), and representative images of SI and small intestinal length (scale bar, 1 cm) (**D**) of the indicated mice fed the specified diet for 2 weeks. (**E**) Eosinophils, total ILC2s, and R5-expressing ILC2s per gram of epididymal white adipose tissue (eWAT) in WT and TKO mice fed the specified diet for 2 weeks. Data represent individual biological replicates and are presented as means ± SD from two or more independent experiments ($n \geq 3$ mice per group). *P* values were calculated by unpaired *t* test [(A), (C), and (D)], one-way ANOVA (B), or two-way ANOVA with Tukey's multiple comparisons test (E). $^{*}P < 0.05$; $^{**}P < 0.01$; $^{***}P < 0.001$; $^{****}P < 0.0001$; ns, not significant.

responded to chitin, inducing expression of the ILC2-activating cytokines *Il25* and *Il33* in stomach tuft cells and nontuft epithelial cells, respectively (Fig. 1C).

Dietary chitin increased stomach IL-5– and IL-13–producing ILC2s (Fig. 1D) and alternatively activated Arg1^{+} macrophages, serum IL-5, and blood eosinophils, whose numbers expanded over time and in proportion with chitin content (fig. S1, C to E). Few IL-5– or IL-13–expressing stomach CD4^{+} T cells were detected, however, and chitin responses were intact in *Rag1* knockout (*Rag1*-KO) mice, which lack B and T cells (fig. S1, F to I), consistent with predominantly innate immune activation. Chitin ingestion increased stomach expression of the gene encoding ILC2-activating neuropeptide neuromedin U (*Nmu*) (*16*, *17*) along with the gene encoding its receptor, *Nmur1*, among stomach-resident ILC2s (fig. S1, J and K). The expression of calcitonin gene–related peptide (CGRP), another ILC2-activating neuropeptide (*18*), was unaltered by dietary chitin (fig. S1L). Thus, gastric ILC2s may be synergistically activated by IL-25 and NMU, similar to intestinal ILC2s (*16*, *17*).

Dietary chitin also increased gastrin and glucagon-like peptide-1 (GLP-1), GI hormones that are induced by mechanical stretch after food ingestion (*19*). By contrast, serotonin, which responds to IL-33 (*20*), was unaffected by chitin (fig. S1, M and N). In addition, although IL-33 can be released by mechanical perturbation (*21*) and drives ILC2 responses to *Helicobacter pylori* infection and chemical injury (*22*, *23*), chitin-induced ILC2 accumulation and eosinophilia were unaffected in *Il1rl1*-KO mice (fig. S2, A and B). By contrast, ILC2 activation and cytokine production was abolished in TKO mice (Fig. 1, C and D), and eosinophilia was abrogated in both tuft cell–deficient *Pou2f3*-KO and TKO mice (fig. S2, C and D), whereas chitin-induced stomach distension was maintained. Thus, tuft cell–derived IL-25 appears to be the primary signal in gastric ILC2 responses to dietary chitin–induced stretch.

We inflated the stomach with air to recapitulate chitin-induced distension (fig. S2E). Within 2 hours, we observed increased expression of *Il25*, *Nmu*, and *Edn1*, which is induced by triggering the mechanosensitive ion channel Piezo1 (*24*, *25*). Conversely, in vivo administration of GsMTx-4, a stretch-activated channel inhibitor, blocked this response (Fig. 1E and fig. S2F) and abrogated ILC2 cytokine induction after chitin ingestion (Fig. 1F). Administration of the Piezo1 agonist Yoda1 induced ILC2 IL-5 production in WT but not TKO mice (Fig. 1G), suggesting that Piezo1 signaling activates gastric ILC2s through tissue cytokines, including IL-25. Accordingly, Yoda1 did not enhance gastric ILC2 responses before tuft cell development (fig. S2, G and H). *Nmur1* expression was reduced in TKO ILC2s compared with WT ILC2s (fig. S2I), which is consistent with prior reports (*16*) and suggests that gastric ILC2s acquire basal IL-5 expression and receptivity to multiple stretch signals during development. Combined Yoda1 and NMU administration also increased ILC2 IL-13 and KLRG1 expression compared with Yoda1 alone (Fig. 1H and fig. S2J). Thus, dietary chitin and mechanical stretch initiates type 2 immune responses that sensitize ILC2s to additional synergistic neuroimmune activating signals.

Sustained chitin intake promotes GI remodeling and adipose ILC2 responses

Dietary chitin remodeled GI tissues, inducing gastric epithelial proliferation, epithelial and submucosal thickening, and increased tuft cell abundance (Fig. 2, A to C). Proliferation was reduced in TKO mice compared with WT mice (Fig. 2B), indicating a requirement for IL-25, IL-33, and TSLP signaling in remodeling. Chitin lengthened the small intestine (SI), which was enriched with tuft cells, activated ILC2s, and eosinophils in WT but not TKO mice (Fig. 2D and fig. S3, A and B). These SI effects closely resembled those induced by helminths, protozoa (*Tritrichomonas* spp.), and increased luminal succinate (*26*–*29*). However, control and chitin-fed mice were *Tritrichomonas*-free, and cecal succinate levels were unaffected by chitin (fig. S3C). Thus, dietary chitin appears to initiate a distinctive type 2 immune circuit within the GI tract.

Chitin intake also stimulated type 2 immune responses in metabolically active tissues. Although lung ILC2s and eosinophils were unaffected by diet (fig. S3, D and E), visceral adipose from chitin-fed mice contained elevated numbers of eosinophils and IL-5–producing ILC2s (Fig. 2E). Inhibiting tissue lymphocyte egress by using the immunomodulator FTY720 reduced circulating ILCs (fig. S3F) but did not alter dietary chitin–induced eosinophil and ILC2 responses (fig. S3, G and H), suggesting that interorgan ILC2 migration did not mediate adipose effects (*30*). By contrast, adipose ILC2 activation and eosinophilia were abrogated in TKO mice (Fig. 2E), indicating that tissue-derived cytokines coordinate local ILC2 responses to chitin. Moreover, mice that lacked the shared signaling receptor for IL-4 and IL-13, IL4Rα, failed to induce stomach ILC2s, tuft cells, SI lengthening, adipose ILC2s, and eosinophils in response to chitin (fig. S3, I to M). ILC depletion in *Rag1*-KO mice impaired chitin-induced gastric ILC2 and tuft cell expansion (fig. S3, N and O), whereas tuft cells expanded normally in both *Il4*-KO and *Il5*-KO mice (fig. S3P), which supports a role for IL-13–producing ILC2s in chitin responses. Finally, GI tissue resilience, which relies on ILC2s and IL-13 in the absence of adaptive immunity (*31*), was enhanced in

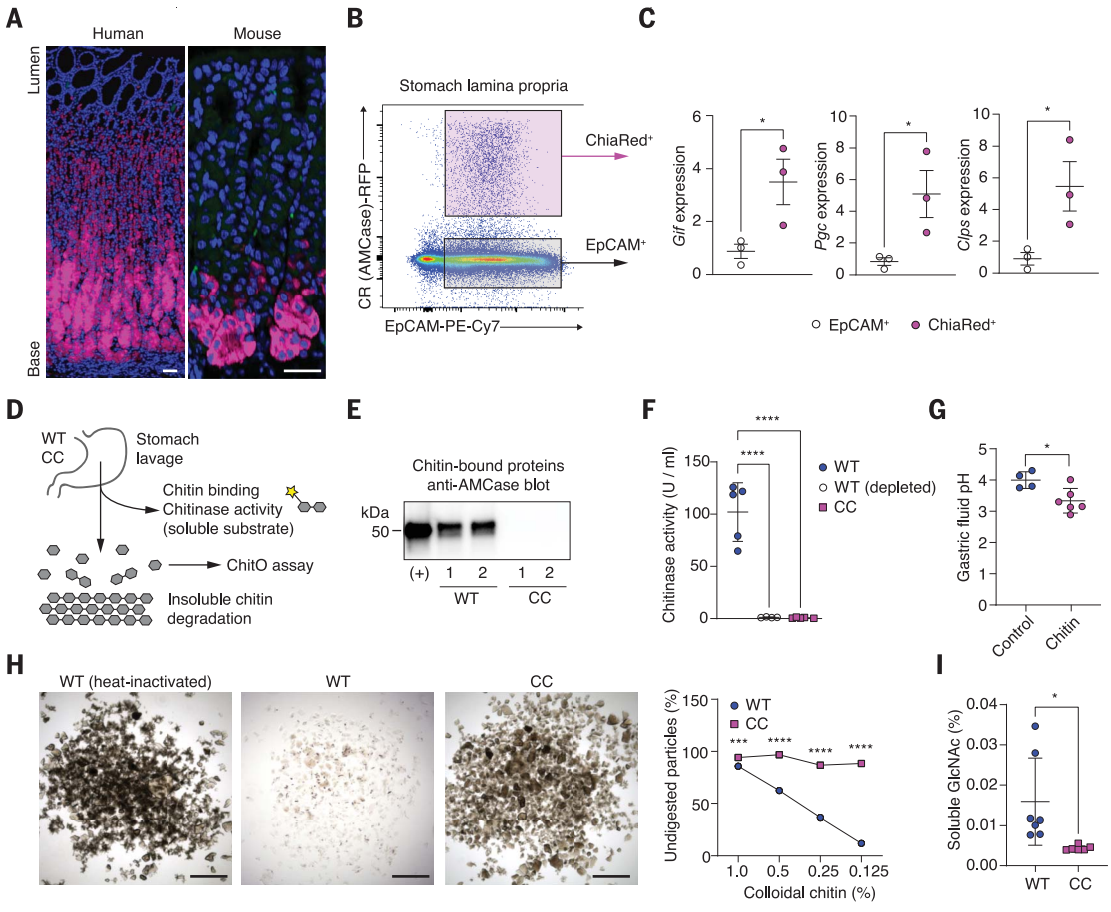

Fig. 3. AMCase is required for dietary chitin digestion. (**A**) Immunostaining of AMCase-expressing chief cells in glandular stomach. Magenta, AMCase; blue, 4′,6-diamidino-2-phenylindole (DAPI); green, autofluorescence (scale bars, 50 μm). Stomach ChiaRed$^+$ (CR: AMCase reporter; CD45$^-$EpCAM$^+$CR$^+$) or total (CD45$^-$EpCAM$^+$CR$^-$) epithelial cells were (**B**) isolated by fluorescence-activated cell sorting and (**C**) analyzed for relative expression of *Gif*, *Clps*, and *Pgc* by quantitative polymerase chain reaction (qPCR. (**D**) Analysis of chitin binding, digestion of soluble chitooligomer and insoluble crystalline chitin substrates, and production of GlcNAc reaction products by chito-oligomer oxidase (ChitO) assay in stomach lavage. (**E**) Immunoblot of chitin-bound AMCase proteins. The "(+)" indicates recombinant AMCase control. (**F**) Chitinase activity with soluble substrate in stomach lavage samples, with and without predepletion of AMCase by using insoluble chitin. (**G**) Gastric fluid pH in mice fasted overnight after 2 weeks on the indicated diet. (**H**) Digestion of insoluble colloidal chitin after 96-hour incubation with inactivated (heat-treated) or fresh stomach lavage from WT or CC mice (scale bars, 500 μm). (**I**) ChitO assay for soluble GlcNAc reaction products in supernatants from insoluble particle digestion in (H). Data points represent individual biological replicates except for the data in (C), which represent samples pooled from three or four mice. Data represent two or more independent experiments ($n \geq 3$ mice per group) and are presented as means ± SD. *P* values were calculated by unpaired *t* test. *$P < 0.05$; ***$P < 0.001$; ****$P < 0.0001$.

chitin-fed *Rag1*-KO mice infected with the helminth *Nippostrongylus brasiliensis* compared with control mice, as marked by increased ILC2s, serum IL-5, and eosinophils and improved worm expulsion (fig. S4, A to D).

Because dietary polysaccharides can be degraded by intestinal bacteria (*7*, *8*, *32*), we profiled the fecal microbiota from chitin- and control diet–fed mice. Mice maintained similar body weights regardless of diet (fig. S5A), which indicates equivalent nutrient extraction. However, chitin intake significantly enriched Bacteroidetes phyla, whereas Firmicutes were proportionally decreased in chitin-fed mice compared with control mice (fig. S5B and table S2). Thus, chitin alters GI bacterial composition, a finding that is consistent with prior work on dietary fiber enrichment (*8*).

We then tested whether type 2 immune responses to dietary chitin were dependent on commensal microbiota using germ-free (GF) and specific-pathogen–free (SPF) mice. GF and SPF mice maintained similar body weights regardless of diet, and dietary chitin induced gastric distension, SI lengthening, eosinophilia, ILC2 expansion, and tuft cell hyperplasia in both the GF and SPF conditions (fig. S5, C to G). These results indicated that dietary chitin induces innate type 2 immune responses independent of commensal microbes. To address possible developmental alterations in GF mice, we also depleted bacteria by administering antibiotics to adult SPF mice before dietary chitin intake. Consistent with GF results, stomach, SI, and adipose tissue chitin responses were unaffected by antibiotics (fig. S5, H to K). Thus, although chitin alters GI microbial composition and commensal microorganisms influence tuft cell succinate responses (*27*, *28*), dietary chitin initiates type 2 immune responses in the absence of commensal microbiota.

Acidic mammalian chitinase is required for dietary chitin digestion in mammals

Chitinases (EC 3.2.1.14) are widely conserved enzymes that cleave soluble chitooligomers and crystalline chitin substrates, liberating *N*-acetylglucosamine (GlcNAc). In contrast to insoluble dietary chitin fibers, GlcNAc did not induce gastric distension or GI type 2 immune responses (fig. S6, A to D), suggesting that undigested, insoluble chitin causes mechanical stretch and type 2 immune triggering. Chitinases can be expressed by microbes, including gut-resident bacteria (*8*). However, the lack of microbial involvement in chitin responses led us to consider acidic mammalian chitinase (AMCase), a mammalian chitinase secreted by respiratory epithelium, salivary glands, and stomach that has been evolutionarily linked to chitin consumption (*10*–*12*, *33*).

AMCase was expressed at the base of gastric glands in tissues from human sleeve-gastrectomy patients and 8-week-old mice (Fig. 3A), which is consistent with RNA sequencing (RNA-seq) data (fig. S7A) and prior reports (*10*, *33*–*35*), which supported chief cells as the main source of AMCase in the mammalian stomach. We further investigated AMCase-expressing cells using ChiaRed reporter mice, in which tdTomato and Cre recombinase are knocked into *Chia1* (which encodes AMCase). Homozygous ChiaRed (CC) mice lack AMCase (*36*). We lineage-traced AMCase-expressing cells by crossing ChiaRed with Rosa26-flox-stop-zsGreen [R26(LSL)-

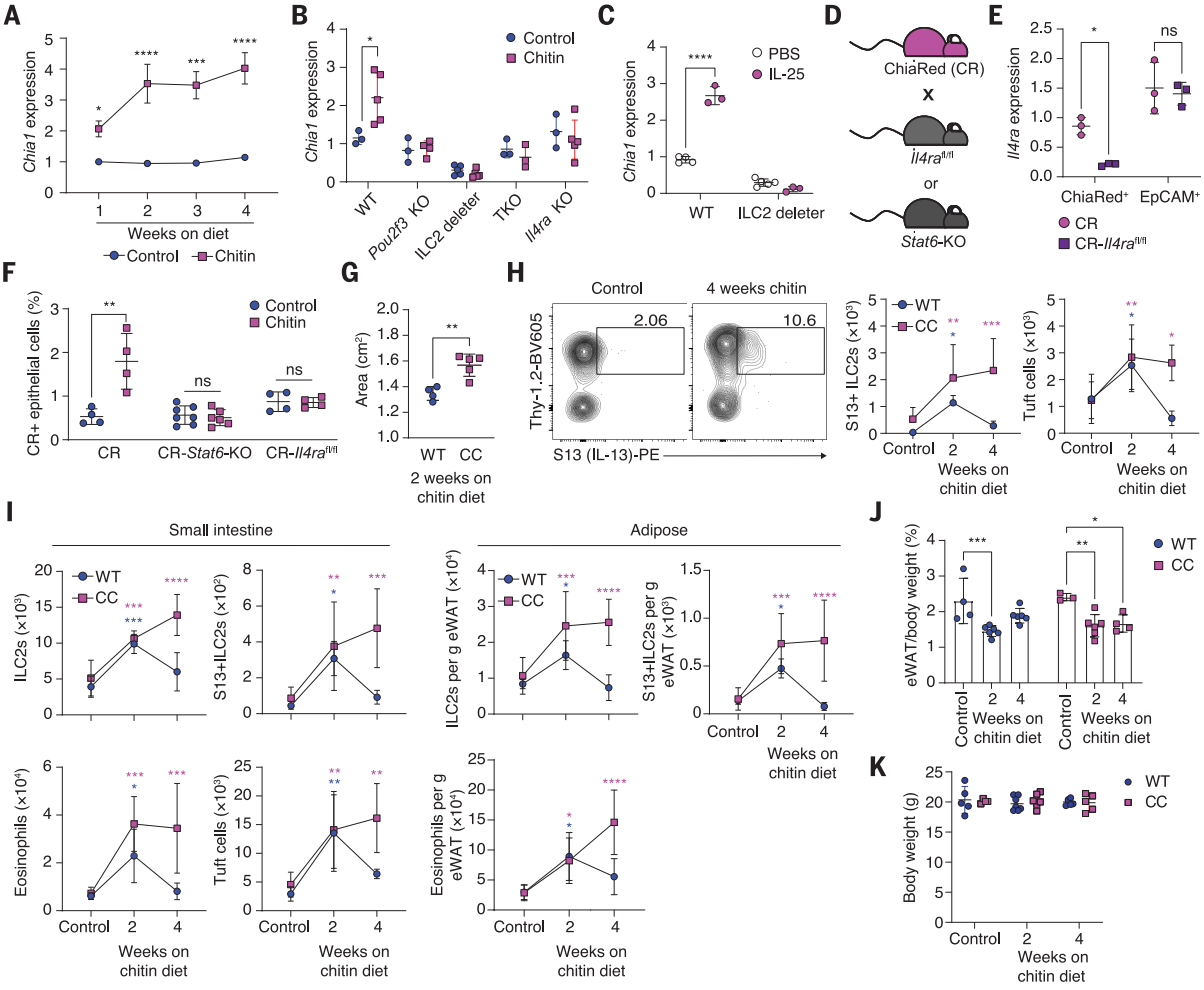

Fig. 4. Stomach adaptation to dietary chitin is controlled by a type 2 immune circuit. Relative *Chia1* stomach expression in WT (**A**) and indicated mouse strains (**B**) after 2 weeks on the indicated diet. (**C**) *Chia1* expression in stomach tissue from WT and ILC2-deficient deleter mice after IL-25 administration. (**D**) Breeding scheme to obtain CR-*Stat6*-KO, and CR-*Il4ra*$^{fl/fl}$ mice. (**E**) Relative *Il4ra* expression in ChiaRed$^+$ or total stomach epithelial cells (EpCAM$^+$) from ChiaRed and CR-*Il4ra*$^{fl/fl}$ mice. (**F**) Percentage of ChiaRed$^+$ (CR) chief cells out of total stomach epithelial cells in ChiaRed, CR-*Il4ra*$^{fl/fl}$, and CR-*Stat6*-KO mice fed the indicated diet for 2 weeks. (**G**) Stomach size of WT and CC mice fed the indicated diet for 2 weeks. S13 (IL-13)–expressing ILC2s and tuft cells in stomach (**H**); SI tuft cells, SI and adipose eosinophils, ILC2s, and S13$^+$ ILC2s (**I**); eWAT-to–body weight ratio (**J**), and body weights (**K**) of WT and CC mice fed control or chitin diets as indicated. Data represent individual biological replicates except for the data in (A), (E), (H), and (I), which are pooled from three to eight mice and are presented as means ± SD from two or more independent experiments ($n \geq 3$ mice per group). *P* values were calculated by unpaired *t* test [(A) to (C) and (E) to (G)] or two-way ANOVA with Tukey's multiple comparisons test [(H) to (K)]. **P* < 0.05; ***P* < 0.01; ****P* < 0.001; *****P* < 0.0001; ns, not significant.

zsGreen] mice. Consistent with antibody staining, AMCase-expressing ChiaRed$^+$zsGreen$^+$ cells were localized in gastric glands and concordantly coexpressed ChiaRed and zsGreen with age (fig. S7B), indicating that AMCase expression is sustained in terminally differentiated chief cells. ChiaRed$^+$ cells were also enriched for mature chief cell markers gastric intrinsic factor (*Gif*), colipase (*Clps*), and pepsinogen C (*Pgc*) (Fig. 3, B and C), which supports AMCase as a marker of zymogenic digestive cells.

We tested the contribution of AMCase to chitin digestion using GI luminal secretions from WT and CC (AMCase-deficient) mice. Chitinase activity was assessed on soluble chitooligomers and crystalline chitin substrates (*37*), and chitin-binding proteins were isolated with magnetized chitin (Fig. 3D). WT stomach lavage contained AMCase that bound insoluble chitin (Fig. 3E) and exhibited robust chitinase activity that was absent in CC lavage and could be depleted by preincubation with chitin (Fig. 3F), which indicates that AMCase binds chitin and nonredundantly mediates stomach chitinase activity. Dietary chitin intake also reduced stomach pH (Fig. 3G), which enhances AMCase enzymatic activity (*10*, *33*) and suggests a coordinated physiological digestion response that involves acid-secreting parietal cells. Crystalline dietary chitin fibers were visibly digested and converted to soluble GlcNAc by WT stomach lavage, which reflects highly efficient chitinase digestive activity. However, this activity was absent in CC lavage, which retained undigested crystalline chitin particles and failed to produce soluble GlcNAc reaction products (Fig. 3, H and I). Neither control nor chitin chow elicited detectable epithelial ChiaRed or *Chia1* expression in lower GI tissues, including SI and cecum (fig. S8, A to C). However, WT SI lavage still contained chitinase activity that was absent in CC SI lavage, suggesting that AMCase produced in the stomach transits into the lower GI tract, where it also makes up the major source of chitinase activity (fig. S8D). Thus, although most insoluble dietary polysaccharides consumed by mammals resist digestion or undergo only limited degradation in the lower GI tract by commensal microbiota–derived glycosyl hydrolases (*7*, *8*), dietary chitin is primarily digested by host-encoded AMCase.

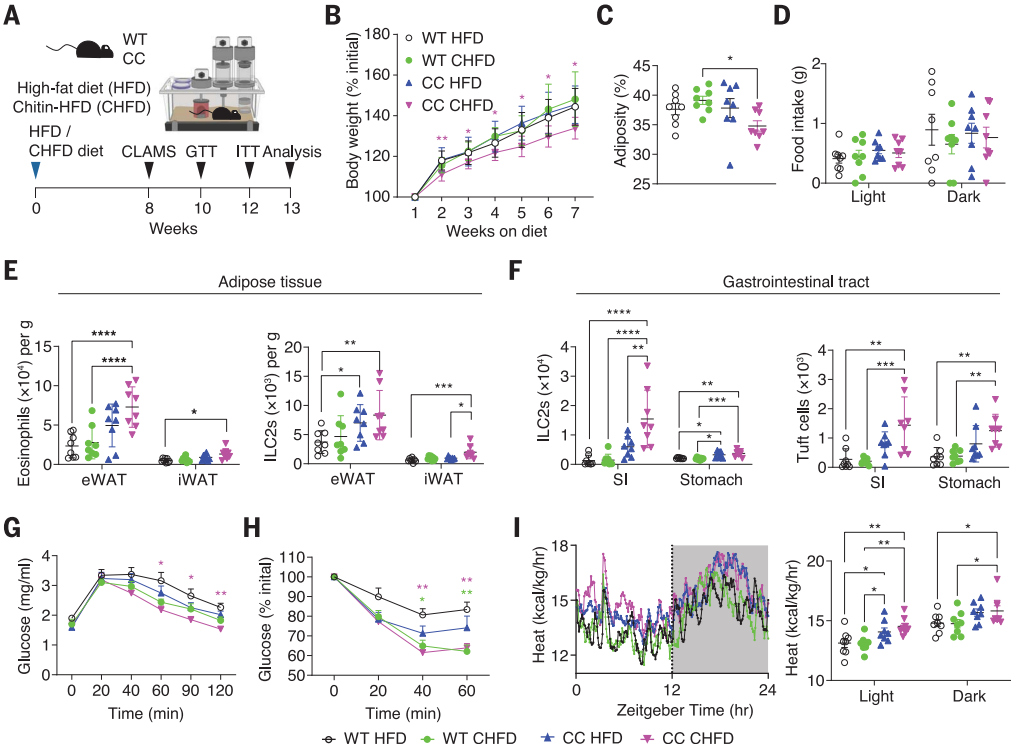

Fig. 5. Dietary chitin improves metabolic health in high-fat diet–induced obesity. (**A**) Experimental design. HFD- or CHFD-fed WT or CC mice were subjected to metabolic cage analyses (CLAMS), glucose tolerance tests (GTTs), and insulin tolerance tests (ITTs). [Part of the illustration was created with Biorender.com] Body weights (**B**), adiposity (**C**), and food intake (24-hour average) (**D**) of WT and CC mice after 8 weeks on the indicated diet. Eosinophils and ILC2s in adipose tissue (**E**) and tuft cells and ILC2s in SI and stomach tissues (**F**) in WT and CC mice after 13 weeks on the indicated diet. iWAT, inguinal white adipose tissue. (**G**) GTT curves at 10 weeks. (**H**) ITT curves at 12 weeks. (**I**) Heat curve and averages over 24 hours in CLAMS cages at 8 weeks. Data represent individual biological replicates except for data in (B), (E), and (F); in these panels, each data point represents eight pooled mice and are presented as means ± SD [(E) and (F)] or means ± SEM [(B) to (D) and (G) to (I)], from two or more independent experiments (n = 8 mice per group). P values were calculated by one-way ANOVA (C), two-way ANOVA [(E) and (F)], or two-way ANOVA with repeated measures [(B), (D), and (G) to (I)] with Tukey's multiple comparisons test. *P < 0.05; **P < 0.01; ***P < 0.001; ****P < 0.0001.

Stomach adaptation to dietary chitin is controlled by a type 2 immune circuit

Because lung AMCase expression is promoted by type 2 cytokines (*36*, *38*), we tested whether stomach AMCase is similarly regulated. Indeed, sustained dietary chitin intake increased *Chia1* expression in WT but not *Il4ra*-KO, *Pou2f3*-KO, ILC2-deleter mice that lack ILC2s (*15*), or TKO mice (Fig. 4, A and B). Tuft cell–derived IL-25, ILC2s, and IL-4Rα signaling were therefore implicated as major drivers of gastric AMCase expression. Type 2 triggering was recapitulated by IL-25 administration, which stimulated IL-13 production by ILC2s and stomach *Chia1* expression in WT but not ILC2-deficient mice (Fig. 4C and fig. S8E). Thus, ILC2-derived IL-13 is implicated in the expansion of AMCase-expressing chief cells.

To test this further, we crossed ChiaRed with *Stat6*-KO (CR-*Stat6*-KO) and *Il4ra*$^{fl/fl}$ mice (*39*) (CR-*Il4ra*$^{fl/fl}$), which enabled specific deletion of IL4Rα from AMCase-expressing cells (Fig. 4D). *Il4ra* was reduced in ChiaRed^{+} stomach epithelial cells from CR-*Il4ra*$^{fl/fl}$ mice compared with ChiaRed controls, indicating successful Cre-mediated excision (Fig. 4E). Dietary chitin increased AMCase-expressing chief cells in WT ChiaRed mice but failed to occur in both CR-*Stat6*-KO and CR-*Il4ra*$^{fl/fl}$ mice (Fig. 4F), indicating that dietary chitin promotes chief cell AMCase expression through cell-intrinsic IL4Rα signaling. We also examined acute gastric injury and transient chief cell depletion by high-dose tamoxifen treatment (HDT), which models aspects of human atrophic corpus gastritis and AMCase loss due to *H. pylori* infection (*40*, *41*). After HDT, WT mice activated gastric ILC2s coincident with chief cell recovery, whereas TKO mice failed to recover *Chia1* (fig. S9, A and B). Thus, restoration of gastric homeostasis and chitin digestive capacity after epithelial injury depends on type 2 circuit activation.

These data suggest that mammals adapt to dietary chitin by inducing endogenous stomach type 2 immune responses to boost AMCase production. Accordingly, CC mice failed to reduce gastric distension compared with WT mice after 2 weeks of chitin intake (Fig. 4G). Stomach ILC2 activation and tuft cell hyperplasia were also sustained in CC versus WT mice over several weeks (Fig. 4H), which reflects unresolved circuit activation without AMCase-catalyzed chitin digestion. Consistent with improved digestion, WT mice attenuated distal type 2 immune triggering in the SI and adipose tissues. CC mice, by contrast, exhibited enhanced and prolonged type 2 triggering, characterized by greater SI tuft cell abundance, increased eosinophils, and increased IL-13–producing ILC2s in SI and adipose tissues after 4 weeks of chitin intake (Fig. 4I). Adipose tissue weight was also reduced in proportion to body weight in CC mice compared with WT mice, whereas body weights were similar (Fig. 4, J and K). Thus, both GI and adipose tissue homeostasis are regulated by the AMCase-mediated adaptation to dietary chitin.

Dietary chitin improves metabolic health in obesity

We next tested the impact of dietary chitin on obesity, which is influenced by neuronal-ILC2 interactions and type 2 cytokines (*3*–*5*, *42*). We fed WT and CC mice isocaloric high-fat diets containing either cellulose (control; HFD) or chitin (CHFD) fiber (Fig. 5A). Food intake was similar among all groups, and HFD-fed mice showed comparable body weight gain. However, CHFD-fed CC mice gained significantly less weight, with reduced adiposity and fat mass compared with WT mice (Fig. 5, B to D, and fig. S10A). Resistance to obesity in CHFD-fed CC mice was accompanied by adipose ILC2 and eosinophil accumulation (Fig. 5E), which have been previously linked with metabolic homeostasis (*3*–*5*), suggesting that altered dietary chitin digestion could modulate metabolism. Indeed, numbers of ILC2s and tuft cells were elevated in the stomach and SI tissues of CHFD-fed CC compared with those of WT mice (Fig. 5F), which reflects sustained type 2 triggering and suggests that AMCase-mediated dietary chitin digestion contributes to metabolic homeostasis.

Both dietary chitin and AMCase influenced metabolism in the context of high-fat diets because CHFD-fed WT and CC mice exhibited significantly improved insulin sensitivity compared with HFD-fed WT mice (Fig. 5, G and H). CHFD-fed CC mice exhibited lower fasting glucose compared with WT mice (fig.

S10B), which is consistent with differences in body weight and suggests that AMCase activity influences glucose homeostasis after chitin ingestion. Additionally, light-phase energy expenditure was increased in CC mice, and the respiratory exchange ratio was increased after CHFD feeding compared with HFD feeding in both WT and CC mice, despite no differences in core body temperature or activity (Fig. 5I and fig. S10, C to E), which is consistent with sustained type 2 immune triggering. Indeed, tuft cell–deficient *Pou2f3*-KO mice failed to exhibit CHFD-induced effects on insulin sensitivity (fig. S11, A to G), suggesting that type 2 circuit initiation is required for some metabolic aspects of chitin in a high-fat diet. Thus, disruption of the mammalian stomach's adaptation to dietary chitin alters nutrient uptake and metabolic homeostasis, which manifests in obesity.

Discussion

Chitin consumption has been linked to *CHIA* gene selection throughout primate evolution (*11*, *12*), and chitin-rich fungi and arthropods are constituents of the diets of both modern and ancient human populations (*13*). Mammalian glycosyl hydrolase gene selection has also been linked with starch consumption (*43*, *44*), but adaptations to specific dietary fibers after ingestion are mainly ascribed to shifts in gut microbial composition. As shown here, mammals encode an endogenous circuit that enables chitin catabolism and nutrient extraction through AMCase production. This pathway is triggered by gastric distension, neuropeptide release, and type 2 cytokine production caused by insoluble chitin fibers, which result in GI remodeling and chief cell AMCase induction over time. This in turn enables enhanced chitin digestion. In humans, *CHIA* variants resulting in lower chitinase activity are linked with asthma (*45*, *46*), which supports dual roles for AMCase in mucosal defense and nutrient extraction, as proposed initially (*33*). AMCase-producing chief cells produce additional digestive enzymes such as pepsinogen and lipase, which suggests that gastric ILC2s may coordinate a response that improves overall digestion of recalcitrant insect or fungal foods, perhaps representing a strategy for omnivores to adapt to varied diets. Although microbial composition is altered in response to chitin and other polysaccharides, we show that the mammalian adaptation does not rely on commensal microbiota and that AMCase is the primary source of chitinase activity in the GI tract, thereby distinguishing chitin digestion from other abundant insoluble polysaccharides such as cellulose. Our results further elucidate a mechanism for how chitin initiates type 2 immune initiation by means of mechanical stretch, thus connecting physical tissue perturbation with a branch of immunity increasingly recognized to maintain homeostasis in response to a wide variety of environmental disruptions as well as neural and dietary fluctuations. Intriguingly, the mammalian adaptation to chitin influences innate resistance to helminth infection and metabolic homeostasis, suggesting that chitin digestive pathways coevolved with intestinal helminths and may represent a therapeutic target in metabolic diseases such as obesity.

REFERENCES AND NOTES

1. J. L. Slavin, *Nutrition* **21**, 411–418 (2005).
2. S. K. Gill, M. Rossi, B. Bajka, K. Whelan, *Nat. Rev. Gastroenterol. Hepatol.* **18**, 101–116 (2021).
3. D. Wu *et al*., *Science* **332**, 243–247 (2011).
4. A. B. Molofsky *et al*., *J. Exp. Med.* **210**, 535–549 (2013).
5. J. R. Brestoff *et al*., *Nature* **519**, 242–246 (2015).
6. N. T. Nguyen, J. E. Varela, *Nat. Rev. Gastroenterol. Hepatol.* **14**, 160–169 (2017).
7. H. J. Flint, K. P. Scott, S. H. Duncan, P. Louis, E. Forano, *Gut Microbes* **3**, 289–306 (2012).
8. J. L. Sonnenburg *et al*., *Science* **307**, 1955–1959 (2005).
9. M. G. Paoletti, L. Norberto, R. Damini, S. Musumeci, *Ann. Nutr. Metab.* **51**, 244–251 (2007).
10. M. Ohno *et al*., *Sci. Rep.* **6**, 37756 (2016).
11. C. A. Emerling, F. Delsuc, M. W. Nachman, *Sci. Adv.* **4**, eaar6478 (2018).
12. M. C. Janiak, M. E. Chaney, A. J. Tosi, *Mol. Biol. Evol.* **35**, 607–622 (2018).
13. M. C. Wibowo *et al*., *Nature* **594**, 234–239 (2021).
14. S. J. Van Dyken *et al*., *Immunity* **40**, 414–424 (2014).
15. S. J. Van Dyken *et al*., *Nat. Immunol.* **17**, 1381–1387 (2016).
16. V. Cardoso *et al*., *Nature* **549**, 277–281 (2017).
17. A. Wallrapp *et al*., *Nature* **549**, 351–356 (2017).
18. P. Sui *et al*., *Science* **360**, eaan8546 (2018).
19. T. Zhang, M. H. Perkins, H. Chang, W. Han, I. E. de Araujo, *Cell* **185**, 2478–2494.e28 (2022).
20. Z. Chen *et al*., *Immunity* **54**, 151–163.e6 (2021).
21. R. Kakkar, H. Hei, S. Dobner, R. T. Lee, *J. Biol. Chem.* **287**, 6941–6948 (2012).
22. N. Satoh-Takayama *et al*., *Immunity* **52**, 635–649.e4 (2020).
23. A. R. Meyer *et al*., *Gastroenterology* **159**, 2077–2091.e8 (2020).
24. A. G. Solis *et al*., *Nature* **573**, 69–74 (2019).
25. Y. Oh *et al*., *Neuron* **109**, 1979–1995.e6 (2021).
26. J. von Moltke, M. Ji, H.-E. Liang, R. M. Locksley, *Nature* **529**, 221–225 (2016).
27. C. Schneider *et al*., *Cell* **174**, 271–284.e14 (2018).
28. W. Lei *et al*., *Proc. Natl. Acad. Sci. U.S.A.* **115**, 5552–5557 (2018).
29. M. S. Nadjsombati *et al*., *Immunity* **49**, 33–41.e7 (2018).
30. Y. Huang *et al*., *Science* **359**, 114–119 (2018).
31. A. E. Price *et al*., *Proc. Natl. Acad. Sci. U.S.A.* **107**, 11489–11494 (2010).
32. P. J. Turnbaugh *et al*., *Nature* **444**, 1027–1031 (2006).
33. R. G. Boot *et al*., *J. Biol. Chem.* **276**, 6770–6778 (2001).
34. M. Suzuki *et al*., *J. Histochem. Cytochem.* **50**, 1081–1089 (2002).
35. X. Han *et al*., *Cell* **172**, 1091–1107.e17 (2018).
36. S. J. Van Dyken *et al*., *Cell* **169**, 497–509.e13 (2017).
37. B. A. Barad *et al*., *Protein Sci.* **29**, 952–977 (2020).
38. T. A. Reese *et al*., *Nature* **447**, 92–96 (2007).
39. D. R. Herbert *et al*., *Immunity* **20**, 623–635 (2004).
40. W. J. Huh *et al*., *Gastroenterology* **142**, 21–24.e7 (2012).
41. I. Nookaew *et al*., *BMC Med. Genomics* **6**, 41 (2013).
42. F. Cardoso *et al*., *Nature* **597**, 410–414 (2021).
43. G. H. Perry *et al*., *Nat. Genet.* **39**, 1256–1260 (2007).
44. E. Axelsson *et al*., *Nature* **495**, 360–364 (2013).
45. M. A. Seibold *et al*., *J. Biol. Chem.* **284**, 19650–19658 (2009).
46. K. Okawa *et al*., *Mol. Biol. Evol.* **33**, 3183–3193 (2016).
47. D. H. Kim *et al*., A type 2 immune circuit in the stomach controls mammalian adaptation to dietary chitin, version 1. Dryad (2023); https://doi.org/10.5061/dryad.12jm63z3m.

ACKNOWLEDGMENTS

We thank K. Ravichandran for comments on the manuscript; J. Mills, R. Locksley, H.-E. Liang, J. Kipnis, M. Baldridge, C. Wilen, and C. Hsieh for advice and reagents; L. Mosby for expert technical assistance; and J. M. White at the Department of Pathology and Immunology Gnotobiotic Facility at Washington University in St. Louis for assistance with GF experiments. **Funding:** This work was supported in part by the Bursky Center for Human Immunology and Immunotherapy Programs, Center for Cellular Imaging, and Rheumatic Diseases Research Resource-based Center (NIH P30 AR073752) at Washington University in St. Louis; NIH DP5 OD028125 (J.R.B.); Burroughs Wellcome Fund CAMS #1019648 (J.R.B.); NIH R01HL148033, R01AI176660, and R21AI163640 (S.J.V.D.); and the National Research Foundation of Korea Award NRF-2020R1A6A3A03037855 (D.-H.K.). **Author contributions:** D.-H.K. and S.J.V.D. designed the study and performed experiments. Y.W. and H.J. performed experiments and provided advice. R.L.F., X.Z., and J.R.B. performed metabolic cage experiments, analyzed data, and provided expertise with metabolic studies. C.M. and T.-C.L. provided human stomach specimens and expertise, and J.S.F. provided biochemical reagents and expertise. All authors edited the final manuscript. S.J.V.D. directed the studies and wrote the manuscript with D.-H.K. **Competing interests:** J.R.B. is on the scientific advisory board of LUCA Science, Inc. The other authors declare that they have no competing interests. **Data and materials availability:** All data are available in the main text or supplementary materials. 16*S* sequencing data are available in Dryad (*47*).

SUPPLEMENTARY MATERIALS

science.org/doi/10.1126/science.add5649
Materials and Methods
Figs. S1 to S11
Tables S1 to S3
References (*48*–*52*)
MDAR Reproducibility Checklist

Submitted 20 June 2022; resubmitted 8 May 2023
Accepted 8 August 2023
10.1126/science.add5649

A type 2 immune circuit in the stomach controls mammalian adaptation to dietary chitin

Do-Hyun Kim, Yilin Wang, Haerin Jung, Rachael L. Field, Xinya Zhang, Ta-Chiang Liu, Changqing Ma, James S. Fraser, Jonathan R. Brestoff, and Steven J. Van Dyken

Science, **381** (6662), .
DOI: 10.1126/science.add5649

Editor's summary

Chitin (#-1,4-poly-*N*-acetylglucosamine) is a highly abundant natural polysaccharide found in arthropods and fungi that can initiate type 2 (allergic) immune responses. Kim *et al*. report in mice that the consumption of chitin triggers gastric distension, downstream neuropeptide release, and type 2 cytokine production by tuft cells and type 2 innate lymphoid cells. This in turn drives gastrointestinal remodeling and the generation of acidic mammalian chitinase by chief cells, which is needed for chitin digestion. The addition of dietary chitin improved metabolic readouts in mice fed a high-fat diet, possibly because activated chief cells produce other digestive enzymes, including lipase. This mammalian adaptation to chitin may therefore serve as a potential therapeutic target for metabolic diseases such as obesity. — Seth Thomas Scanlon

Science (ISSN) is published by the American Association for the Advancement of Science. 1200 New York Avenue NW, Washington, DC 20005. The title *Science* is a registered trademark of AAAS.